The Fröhlich-Coulomb model of high-temperature superconductivity and charge segregation in the cuprates

2002 J. Phys.: Condens. Matter 14 5337

(http://iopscience.iop.org/0953-8984/14/21/308)

INSTITUTE OF PHYSICS PUBLISHING JOURNAL OF PHYSICS: CONDENSED MATTER

J. Phys.: Condens. Matter **14** (2002) 5337–5348 PII: S0953-8984(02)34885-9

The Fröhlich–Coulomb model of high-temperature superconductivity and charge segregation in the cuprates

A S Alexandrov[1] **and P E Kornilovitch**[2]

[1] Department of Physics, Loughborough University, Loughborough LE11 3TU, UK
[2] Hewlett Packard Labs, 1501 Page Mill Road 1L-1123, Palo Alto, CA 94304, USA

Received 14 March 2002
Published 16 May 2002
Online at stacks.iop.org/JPhysCM/14/5337

Abstract

We introduce a generic Fröhlich–Coulomb model of the oxides, which also includes infinite on-site (Hubbard) repulsion, and describe a simple analytical method of solving the multi-polaron problem in complex lattice structures. Two particular lattices, a zigzag ladder and a perovskite layer, are studied. We find that, depending on the relative strength of the Fröhlich and Coulomb interactions, these systems are either polaronic Fermi (or Luttinger) liquids, bipolaronic superconductors, or charge-segregated insulators. In the superconducting phase the carriers are superlight mobile bipolarons. The model describes key features of the cuprates such as their T_c-values, the isotope effects, the normal-state diamagnetism, the pseudogap, and spectral functions measured in tunnelling and photoemission. We argue that a low Fermi energy and strong coupling of carriers with high-frequency phonons is the cause of high critical temperatures in novel superconductors.

(Some figures in this article are in colour only in the electronic version)

There is overwhelming experimental [1–6] and theoretical [7–10] evidence for an exceptionally strong electron–phonon (el–ph) interaction in the cuprates, which competes with electron correlations. In recent years, several publications addressed the fundamental problem of competing el–ph and Coulomb interactions in the framework of the so-called Holstein–Hubbard model [11–15], where both interactions are short range (on-site). The model describes well many properties of the insulating state of the cuprates, including antiferromagnetism, lattice distortions, and phase segregation. However, it could hardly account for the high value of the superconducting critical temperature [16]. The mass of (bi)polaronic carriers in this model is very large in the relevant parameter region, and T_c is suppressed below the Kelvin scale.

0953-8984/02/215337+12$30.00

In choosing the correct interaction for high-temperature superconductors (HTSC), we take into account that most of the novel superconductors are doped insulators with highly polarizable ionic lattices. The low density of mobile carriers is unable to screen effectively the direct Coulomb electron–ion and electron–electron interactions. The layered structure of the cuprates reduces screening even further. Since the mobile carriers are confined to the copper–oxygen planes their interaction with out-of-plane ions, such as the apical oxygens, is particularly strong. A parameter-free estimate of the polaron binding energy E_p in the cuprates puts it at about 0.5 eV or larger [17]. This strong long-range (Fröhlich) el–ph interaction necessarily leads to formation of small polarons. Such Fröhlich small polarons were first considered in [18]. Exact Monte Carlo simulations of the single-polaron problem [19] showed that a long-range el–ph interaction effectively removes the difficulty with a large polaron (and bipolaron) mass in the Holstein-type el–ph models. Indeed, the polaron is heavy because it has to carry a lattice deformation with it which is the same deformation as forms the polaron itself. Therefore, there exists a generic relation between E_p and the renormalization of its mass: $m \propto \exp(\gamma E_p/\omega)$, where ω is a characteristic phonon frequency and $\gamma \sim 1$ is a numerical coefficient whose actual value depends on the radius of the interaction. For a short-range el–ph interaction (Holstein) the *entire* lattice deformation disappears and then forms in a new place when the polaron moves between the nearest lattice sites. Therefore, $\gamma = 1$ and the polaron is very heavy for the characteristic cuprates values $E_p \sim 0.5$ eV and $\omega \sim 0.05$ eV. In the case of a long-range interaction, only a fraction of the total deformation changes every time the polaron moves and γ could be as small as 0.25 [16]. Clearly, this results in a dramatic mass reduction since γ enters the exponent. Thus the effective mass could be $\leqslant 10\, m_e$ where a naive Holstein-like estimate would yield a huge mass $\sim 10\,000\, m_e$. The above qualitative reasoning was fully confirmed by analytical [16] and numerical (approximation-free Monte Carlo) [19] studies of the double-chain and double-plane models with long-range el–ph interactions. Later the single-polaron and bipolaron cases of the chain model were analysed in more detail, in [20] and [21], respectively. These studies confirmed a much lower mass of both polaron and bipolaron in comparison to the Holstein–Hubbard limit.

Here we argue that a consistent theory of HTSC must include both the long-range Coulomb repulsion between the carriers and the strong long-range el–ph interaction. We propose an analytically solvable multi-polaron model of high-temperature superconductivity that includes these realistic long-range interactions. From the theoretical standpoint, the long-range Coulomb repulsion is critical in ensuring that the carriers would not form large clusters. Indeed, in order to form stable *pairs* (bipolarons) the el–ph interaction has to be strong enough to overcome the Coulomb repulsion at short distances. Since the el–ph interaction is long range, there is a potential possibility for clustering. We shall demonstrate that the inclusion of the Coulomb repulsion V_c makes the clusters unstable. More precisely, there is a certain window of V_c/E_p inside which the clusters are unstable but bipolarons nonetheless form. In this parameter window the bipolarons are light and the system is a superconductor with a high critical temperature. The bipolarons repel each other and propagate in a band of about the same bandwidth as the single-polaron bandwidth, in sharp contrast with all bipolaronic models considered previously. At a weaker Coulomb interaction the system is a charge-segregated insulator. At a stronger Coulomb repulsion the system is a polaron Fermi (or Luttinger) liquid. In the superconducting phase but close to the clustering boundary, dynamical formation of short-lived clusters or stripes could be expected.

Our generic Fröhlich–Coulomb model explicitly includes the electron kinetic energy, the infinite-range Coulomb and el–ph interactions, as well as the lattice energy. The implicitly present infinite Hubbard U prohibits double occupancy and removes the need to distinguish the fermionic spin. Introducing spinless fermion operators c_n and phonon operators $d_{m\alpha}$, the

model Hamiltonian is written as

$$H = -\sum_{n\neq n'} T(\boldsymbol{n}-\boldsymbol{n}')c_n^\dagger c_{n'} + \sum_{n\neq n'} V_c(\boldsymbol{n}-\boldsymbol{n}')c_n^\dagger c_n c_{n'}^\dagger c_{n'} - \omega\sum_{nm} g_\alpha(\boldsymbol{m}-\boldsymbol{n})(\boldsymbol{e}_{m\alpha}\cdot\boldsymbol{u}_{m-n})c_n^\dagger c_n(d_{m\alpha}^\dagger + d_{m\alpha}) + \omega\sum_{m\alpha}(d_{m\alpha}^\dagger d_{m\alpha} + \tfrac{1}{2}). \tag{1}$$

We note that the el–ph term is written in real rather than momentum space. This is more convenient in working with complex lattices. Here $\boldsymbol{e}_{m\alpha}$ is the polarization vector of αth vibration coordinate at site $\boldsymbol{m}$, $\boldsymbol{u}_{m-n} \equiv (\boldsymbol{m}-\boldsymbol{n})/|\boldsymbol{m}-\boldsymbol{n}|$ is the unit vector in the direction from electron $\boldsymbol{n}$ to the ion $\boldsymbol{m}$, and $g_\alpha(\boldsymbol{m}-\boldsymbol{n})$ is the dimensionless el–ph coupling function. ($g_\alpha(\boldsymbol{m}-\boldsymbol{n})$ is proportional to the *force* acting between $\boldsymbol{m}$ and $\boldsymbol{n}$). We assume that all the phonon modes are dispersionless with frequency ω and that the electrons do not interact with displacements of their own atoms, $g_\alpha(0) \equiv 0$. We also use $\hbar = 1$ throughout the paper.

In general, the many-body model (1) is of considerable complexity. However, we are interested in the limit of strong el–ph interaction. In this case, the kinetic energy is a perturbation and the model can be grossly simplified in a two-step procedure. On the first step, the Lang–Firsov canonical transformation [22] is performed, which diagonalizes the last three terms in equation (1). Introducing $S = \sum_{mn\alpha} g_\alpha(\boldsymbol{m}-\boldsymbol{n})(\boldsymbol{e}_{m\alpha}\cdot\boldsymbol{u}_{m-n})c_n^\dagger c_n(d_{m\alpha}^\dagger - d_{m\alpha})$, one obtains the transformed Hamiltonian without an explicit el–ph term:

$$\tilde{H} = \mathrm{e}^{-S}H\mathrm{e}^{S} = -\sum_{n\neq n'}\hat{\sigma}_{nn'}c_n^\dagger c_{n'} + \omega\sum_{m\alpha}(d_{m\alpha}^\dagger d_{m\alpha} + \tfrac{1}{2}) + \sum_{n\neq n'} v(\boldsymbol{n}-\boldsymbol{n}')c_n^\dagger c_n c_{n'}^\dagger c_{n'} - E_p\sum_n c_n^\dagger c_n. \tag{2}$$

The last term describes the energy which polarons gain due to el–ph interaction. E_p is the familiar polaron (Franck–Condon) shift

$$E_p = \omega\sum_{m\alpha} g_\alpha^2(\boldsymbol{m}-\boldsymbol{n})(\boldsymbol{e}_{m\alpha}\cdot\boldsymbol{u}_{m-n})^2, \tag{3}$$

which we assume to be independent of $\boldsymbol{n}$. E_p is a natural measure of the strength of the el–ph interaction. The third term in equation (2) is the polaron–polaron interaction:

$$v(\boldsymbol{n}-\boldsymbol{n}') = V_c(\boldsymbol{n}-\boldsymbol{n}') - V_{\mathrm{pa}}(\boldsymbol{n}-\boldsymbol{n}'), \tag{4}$$

$$V_{\mathrm{pa}}(\boldsymbol{n}-\boldsymbol{n}') = 2\omega\sum_{m\alpha} g_\alpha(\boldsymbol{m}-\boldsymbol{n})g_\alpha(\boldsymbol{m}-\boldsymbol{n}')(\boldsymbol{e}_{m\alpha}\cdot\boldsymbol{u}_{m-n})(\boldsymbol{e}_{m\alpha}\cdot\boldsymbol{u}_{m-n'}), \tag{5}$$

where V_{pa} is the interpolaron *attraction* due to joint interaction with the same vibrating atoms. Finally, the first term in equation (2) contains the transformed hopping operator $\hat{\sigma}_{nn'}$:

$$\hat{\sigma}_{nn'} = T(\boldsymbol{n}-\boldsymbol{n}')\exp\Bigg[\sum_{m\alpha}[g_\alpha(\boldsymbol{m}-\boldsymbol{n})(\boldsymbol{e}_{m\alpha}\cdot\boldsymbol{u}_{m-n}) - g_\alpha(\boldsymbol{m}-\boldsymbol{n}')(\boldsymbol{e}_{m\alpha}\cdot\boldsymbol{u}_{m-n'})](d_{m\alpha}^\dagger - d_{m\alpha})\Bigg]. \tag{6}$$

At large $E_p/T(\boldsymbol{n}-\boldsymbol{n}')$ this term is a perturbation. In the first order of the strong-coupling perturbation theory [7], $\hat{\sigma}_{nn'}$ should be averaged over phonons because there is no coupling between polarons and phonons in the unperturbed Hamiltonian (the last three terms in equation (2)). For temperatures lower than ω, the result is

$$t(\boldsymbol{n}-\boldsymbol{n}') \equiv \langle\hat{\sigma}_{nn'}\rangle_{ph} = T(\boldsymbol{n}-\boldsymbol{n}')\exp[-G^2(\boldsymbol{n}-\boldsymbol{n}')], \tag{7}$$

$$G^2(\boldsymbol{n}-\boldsymbol{n}') = \sum_{m\alpha} g_\alpha(\boldsymbol{m}-\boldsymbol{n})(\boldsymbol{e}_{m\alpha}\cdot\boldsymbol{u}_{m-n}) \times [g_\alpha(\boldsymbol{m}-\boldsymbol{n})(\boldsymbol{e}_{m\alpha}\cdot\boldsymbol{u}_{m-n}) - g_\alpha(\boldsymbol{m}-\boldsymbol{n}')(\boldsymbol{e}_{m\alpha}\cdot\boldsymbol{u}_{m-n'})]. \tag{8}$$

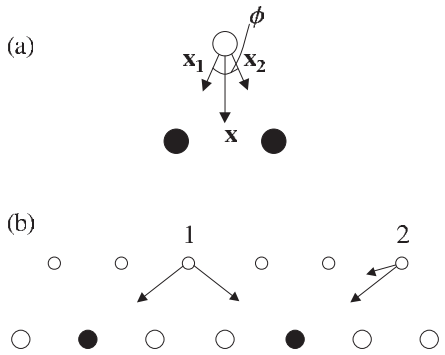

Figure 1. The mechanism of the polaron–polaron interaction. (a) Together, the two polarons (solid circles) deform the lattice more effectively than separately. An effective attraction occurs when the angle ϕ between $\boldsymbol{x}_1$ and $\boldsymbol{x}_2$ is $<\pi/2$. (b) A mixed situation. Atom **1** results in repulsion between two polarons while atom **2** results in attraction.

By comparing equations (3) and (5) with (8), the mass renormalization exponents can be expressed via E_p and $V_{\rm pa}$ as follows:

$$G^2(\boldsymbol{n}-\boldsymbol{n}') = \frac{1}{\omega}\left(E_p - \frac{1}{2}V_{\rm pa}(\boldsymbol{n}-\boldsymbol{n}')\right). \tag{9}$$

This results in a renormalized hopping term that represents the small parameter of a strong-coupling perturbation theory [7]. The above technical transformation is simple and has been described elsewhere [7] together with a detailed description of the perturbation procedure. The resulting model is purely polaronic, in which phonons are 'integrated out':

$$H_p = H_0 + H_{\rm pert}, \tag{10}$$

$$H_0 = -E_p \sum_{\boldsymbol{n}} c^\dagger_{\boldsymbol{n}} c_{\boldsymbol{n}} + \sum_{\boldsymbol{n}\neq\boldsymbol{n}'} v(\boldsymbol{n}-\boldsymbol{n}') c^\dagger_{\boldsymbol{n}} c_{\boldsymbol{n}} c^\dagger_{\boldsymbol{n}'} c_{\boldsymbol{n}'}, \tag{11}$$

$$H_{\rm pert} = -\sum_{\boldsymbol{n}\neq\boldsymbol{n}'} t(\boldsymbol{n}-\boldsymbol{n}') c^\dagger_{\boldsymbol{n}} c_{\boldsymbol{n}'}. \tag{12}$$

When $V_{\rm pa}$ exceeds V_c the full interaction becomes negative and polarons form pairs. We emphasize that while the above formalism fails in some regimes of the short-range el–ph models (for instance, the adiabatic limit of the Holstein model), it is surprisingly accurate for long-range el–ph interactions, as was demonstrated by comparing the analytical results with exact quantum Monte Carlo data [19]. It makes theoretical analysis of even complex interactions and lattice geometries simple and instructive. But before proceeding to analysing concrete lattices, let us elaborate on the physics behind the lattice sums in equations (3) and (5).

When a carrier (electron or hole) acts on an ion with a force $\boldsymbol{f}$, it displaces the ion by some vector $\boldsymbol{x} = \boldsymbol{f}/s$. Here s is the ion's force constant. The total energy of the carrier–ion pair is $-\boldsymbol{f}^2/(2s)$. This is precisely the summand in equation (3) expressed via dimensionless coupling constants. Now, consider two carriers interacting with the *same* ion; see figure 1(a). The ion displacement is $\boldsymbol{x} = (\boldsymbol{f}_1 + \boldsymbol{f}_2)/s$ and the energy is $-\boldsymbol{f}_1^2/(2s) - \boldsymbol{f}_2^2/(2s) - (\boldsymbol{f}_1 \cdot \boldsymbol{f}_2)/s$. The last term here should be interpreted as an ion-mediated interaction between the two carriers. It depends on the scalar product of $\boldsymbol{f}_1$ and $\boldsymbol{f}_2$ and consequently on the relative positions of the carriers with respect to the ion. If the ion is an isotropic harmonic oscillator, as we assume in this paper, then the following simple rule applies. If the angle ϕ between $\boldsymbol{f}_1$ and $\boldsymbol{f}_2$ is $<\pi/2$, then the polaron–polaron interaction is attractive; otherwise it is repulsive; see

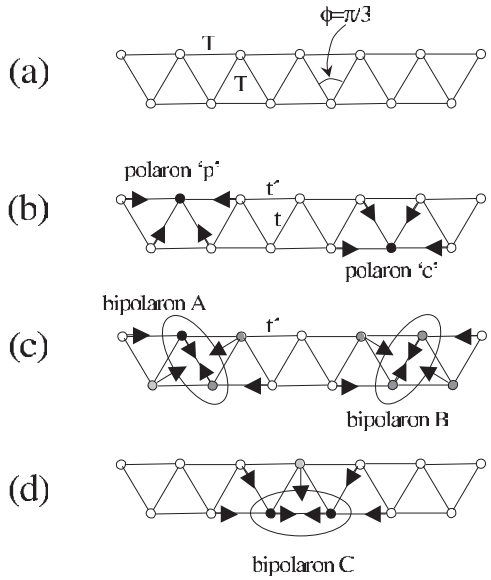

Figure 2. The one-dimensional zigzag ladder. (a) The initial ladder with the bare hopping amplitude T. (b) Two types of polaron with their respective deformations. (c) The two degenerate bipolaron configurations A and B. (d) A different bipolaron configuration C whose energy is higher than that of A and B.

figure 1(b). The overall sign and magnitude of the interaction is given by the lattice sum in equation (5), evaluation of which is elementary. Notice also that according to equation (9), an attractive interaction reduces the polaron mass (and consequently bipolaron mass), while repulsive interaction enhances the mass. Thus in our model the long-range character of the el–ph interaction serves a double purpose. Firstly, it generates additional interpolaron attraction because the distant ions have small angles ϕ. This additional attraction helps overcome the direct Coulomb repulsion between the polarons. Secondly, the Fröhlich interaction makes the bipolarons light, leading to a high critical temperature.

The many-particle ground state of H_0 depends on the sign of the polaron–polaron interaction, the carrier density, and the lattice geometry. First we consider the zigzag ladder, figure 2(a), assuming that all sites are isotropic two-dimensional harmonic oscillators. For simplicity, we also adopt the nearest-neighbour approximation for both interactions, $g_\alpha(\boldsymbol{l}) \equiv g$, $V_c(\boldsymbol{n}) \equiv V_c$, and for the hopping integrals, $T(\boldsymbol{m}) = T_{NN} > 0$ for $l = n = m = a$, and zero otherwise. Hereafter we set the lattice period $a = 1$. There are four nearest neighbours in the ladder; $z = 4$. The one-particle polaronic Hamiltonian takes the form

$$H_p = -\sum_n (E_p[c_n^\dagger c_n + p_n^\dagger p_n] + t'[c_{n+1}^\dagger c_n + p_{n+1}^\dagger p_n + \text{h.c.}] + t[p_n^\dagger c_n + p_{n-1}^\dagger c_n + \text{h.c.}]), \qquad (13)$$

where c_n and p_n are polaronic operators on the lower and upper sides of the ladder, respectively; see figure 2(b). Applying the general formulae (3), (5), and (9), we obtain $E_p = 4g^2\omega$, $t' = T_{NN}\exp[-7E_p/(8\omega)]$, and $t = T_{NN}\exp[-3E_p/(4\omega)]$. Fourier transformation yields the one-particle spectrum

$$E_1(k) = -E_p - 2t'\cos(k) \pm t\cos(k/2). \qquad (14)$$

Two overlapping polaronic bands have a combined width of $W = 4t' + 2t$. The lower band has the bandwidth W and the effective mass $m_l^* = 2/(4t'+t)$ near the bottom, while the upper band has the bandwidth $4t' - 2t$ and a heavier mass $m_u^* = 2/(4t' - t)$.

Let us now place two polarons on the ladder. The nearest-neighbour interaction, equation (4), is found as $v = V_c - E_p/2$ if two polarons are on different sides of the ladder, and $v = V_c - E_p/4$ if both polarons are on the same side. The attractive interaction is provided via the displacement of the lattice sites which are the common nearest neighbours to both polarons, under the condition that the angle ϕ between the directions pointing from those sites to the two polarons is $<\pi/2$. There are two such nearest neighbours for the intersite bipolarons of type A or B (figure 2(c)), but there is only one common nearest neighbour for the bipolaron C (figure 2(d)). When $V_c > E_p/2$, there are no bound states and the multi-polaron system is a 1D Luttinger liquid. However, when $V_c < E_p/2$ and consequently $v < 0$, the two polarons are bound into an intersite bipolaron of type A or B.

It is quite remarkable that the bipolaron tunnelling appears already in the first order in polaron hopping $H_{\rm pert}$ as was anticipated in [16]. This case is different from both that of the on-site bipolaron discussed a long time ago [23], and that of the intersite chain bipolaron discussed recently [21], where the bipolaron tunnelling was of the second order in t. Indeed, in the first order in $H_{\rm pert}$ one should consider only the lowest-energy degenerate configurations A and B and discard the processes that involve all other configurations. The result of such a projection is a bipolaronic Hamiltonian:

$$H_b = (V_c - \tfrac{5}{2}E_p)\sum_n [A_n^\dagger A_n + B_n^\dagger B_n] - t'\sum_n [B_n^\dagger A_n + B_{n-1}^\dagger A_n + \text{h.c.}], \quad (15)$$

where $A_n = c_n p_n$ and $B_n = p_n c_{n+1}$. Fourier transformation yields the bipolaron energy spectrum:

$$E_2(k) = V_c - \tfrac{5}{2}E_p \pm 2t'\cos(k/2). \quad (16)$$

There are two bipolaron bands with a combined width of $4t'$. The bipolaron binding energy is

$$\Delta \equiv 2E_1(0) - E_2(0) = \frac{E_p}{2} - V_c - 2t - 4t'. \quad (17)$$

The bipolaron mass near the bottom of the lowest band is $m^{**} = 2/t'$. Neglecting t and t' relative to E_p and V_c we arrive at the following conclusion. When $V_c < E_p/2$, two polarons form a bipolaron with effective mass $m^{**} \approx (4 + \exp\frac{E_p}{8\omega})m_l^*$. The numerical coefficient $\frac{1}{8}$ ensures that m^{**} remains of the order of m^* even at large E_p.

In models with strong intersite attraction there is a possibility of clustering. In a way similar to the two-particle case above, the lowest energy of n polarons placed on the nearest neighbours of the ladder is found as $E_n = (2n-3)V_c - \frac{6n-1}{4}E_p$, for any $n \geqslant 3$. There are *no* resonating states for an n-polaron nearest-neighbour configuration if $n \geqslant 3$. Therefore there is no first-order kinetic energy contribution to their energy. E_n should be compared with the energy $E_1 + (n-1)E_2/2$ of $(n-1)/2$ widely separated bipolarons and a single polaron for odd $n \geqslant 3$, or with the energy of n widely separated bipolarons for even $n \geqslant 4$. 'Odd' clusters are stable at $V_c < \frac{n}{6n-10}E_p$, and 'even' cluster are stable at $V_c < \frac{n-1}{6n-12}E_p$. Here we have neglected the kinetic energy of polarons and bipolarons. As a result, we find that bipolarons repel each other and single polarons at $V_c > \frac{3}{8}E_p$. If V_c is $<\frac{3}{8}E_p$, then immobile bound clusters of three and more polarons could form. We would like to stress that at distances much larger than the lattice constant the polaron–polaron interaction is always repulsive [16], and the formation of infinite clusters, stripes, or strings is impossible [24]. Combining the condition of bipolaron formation and that of the instability of larger clusters, we obtain a window of parameters:

$$\tfrac{3}{8}E_p < V_c < \tfrac{1}{2}E_p, \quad (18)$$

within which the ladder is a bipolaronic conductor. Outside this window the ladder is either a charge-segregated insulator (small V_c) or a one-dimensional (1D) Luttinger liquid (large V_c).

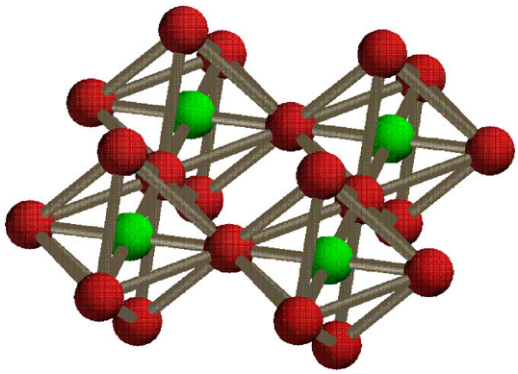

Figure 3. A fragment of the perovskite layer.

Our consideration is directly related to doped cuprates. Here we consider a two-dimensional lattice of ideal octahedra that can be regarded as a simplified model of the copper–oxygen perovskite layer; see figure 3. The lattice period is $a = 1$ and the distance between the apical sites and the central plane is $h = a/2 = 0.5$. All in-plane atoms, both copper and oxygen, are static, but apical oxygens are independent three-dimensional isotropic harmonic oscillators. Because of poor screening, the hole–apical interaction is purely Coulombic, $g_\alpha(\boldsymbol{m}-\boldsymbol{n}) = \kappa_\alpha/|\boldsymbol{m}-\boldsymbol{n}|^2$, $\alpha = x, y, z$. To account for the experimental fact that z-polarized phonons couple with the holes more strongly than the others [3], we choose $\kappa_x = \kappa_y = \kappa_z/\sqrt{2}$. The direct hole–hole repulsion is $V_c(\boldsymbol{n}-\boldsymbol{n}') = \frac{V_c/\sqrt{2}}{|\boldsymbol{n}-\boldsymbol{n}'|}$, so the repulsion between two holes in the NN configuration is V_c. We also include the bare NN hopping T_{NN}, the next-nearest-neighbour (NNN) hopping across copper T_{NNN}, and the NNN hopping between the pyramids T'_{NNN}. According to equation (3), the polaron shift is given by the lattice sum (after summation over polarizations):

$$E_p = 2\kappa_x^2\omega\sum_{\boldsymbol{m}}\left(\frac{1}{|\boldsymbol{m}-\boldsymbol{n}|^4}+\frac{h^2}{|\boldsymbol{m}-\boldsymbol{n}|^6}\right) = 31.15\kappa_x^2\omega, \tag{19}$$

where the factor 2 accounts for the two layers of apical sites. (For reference, the Cartesian coordinates are $\boldsymbol{n} = (n_x+1/2, n_y+1/2, 0)$, $\boldsymbol{m} = (m_x, m_y, h)$; n_x, n_y, m_x, m_y being integers.) The polaron–polaron attraction is

$$V_{\rm pa}(\boldsymbol{n}-\boldsymbol{n}') = 4\omega\kappa_x^2\sum_{\boldsymbol{m}}\frac{h^2+(\boldsymbol{m}-\boldsymbol{n}')\cdot(\boldsymbol{m}-\boldsymbol{n})}{|\boldsymbol{m}-\boldsymbol{n}'|^3|\boldsymbol{m}-\boldsymbol{n}|^3}. \tag{20}$$

Performing the lattice summations for the NN, NNN, and NNN′ configurations one finds $V_{\rm pa} = 1.23E_p$, $0.80E_p$, and $0.82E_p$, respectively. Substituting these results in equations (4) and (9) we obtain the full interpolaron interaction: $v_{NN} = V_c - 1.23E_p$, $v_{NNN} = V_c/\sqrt{2} - 0.80E_p$, $v'_{NNN} = V_c/\sqrt{2} - 0.82E_p$, and the mass renormalization exponents: $G^2_{NN} = 0.38(E_p/\omega)$, $G^2_{NNN} = 0.60(E_p/\omega)$, and $G'^2_{NNN} = 0.59(E_p/\omega)$.

Let us now discuss different regimes of the model. At $V_c > 1.23E_p$, no bipolarons are formed and the system is a polaronic Fermi liquid. The polarons tunnel in the *square* lattice with NN hopping $t = T_{NN}\exp(-0.38E_p/\omega)$ and NNN hopping $t' = T_{NNN}\exp(-0.60E_p/\omega)$. (Since $G^2_{NNN} \approx G'^2_{NNN}$ one can neglect the difference between NNN hoppings within and between the octahedra.) The single-polaron spectrum is therefore

$$E_1(\boldsymbol{k}) = -E_p - 2t'[\cos k_x + \cos k_y] - 4t\cos(k_x/2)\cos(k_y/2). \tag{21}$$

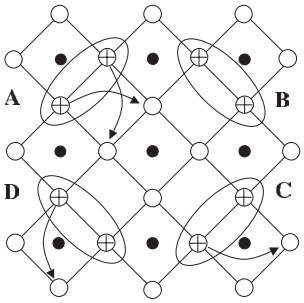

Figure 4. Four degenerate bipolaron configurations A, B, C, and D. Some single-polaron hoppings are indicated by arrows.

The polaron mass is $m^* = 1/(t + 2t')$. Since in general $t > t'$, the mass is mostly determined by the NN hopping amplitude t. If $V_c < 1.23E_p$, then intersite NN bipolarons form. The bipolarons tunnel in the plane via four resonating (degenerate) configurations A, B, C, and D; see figure 4. In the first order in $H_{\rm pert}$ one should retain only these lowest-energy configurations and discard all the processes that involve configurations with higher energies. The result of such a projection is a bipolaron Hamiltonian:

$$\begin{aligned} H_b = (V_c - 3.23E_p) &\sum_l [A_l^\dagger A_l + B_l^\dagger B_l + C_l^\dagger C_l + D_l^\dagger D_l] \\ &- t' \sum_l [A_l^\dagger B_l + B_l^\dagger C_l + C_l^\dagger D_l + D_l^\dagger A_l + \text{h.c.}] \\ &- t' \sum_n [A_{l-x}^\dagger B_l + B_{l+y}^\dagger C_l + C_{l+x}^\dagger D_l + D_{l-y}^\dagger A_l + \text{h.c.}], \end{aligned} \tag{22}$$

where $\boldsymbol{l}$ numbers octahedra rather than individual sites, $\boldsymbol{x} = (1, 0)$, and $\boldsymbol{y} = (0, 1)$. A Fourier transformation and diagonalization of a 4×4 matrix yield the bipolaron spectrum:

$$E_2(\boldsymbol{k}) = V_c - 3.23E_p \pm 2t'[\cos(k_x/2) \pm \cos(k_y/2)]. \tag{23}$$

There are four bipolaronic subbands combined in a band of width $8t'$. The effective mass of the lowest band is $m^{**} = 2/t'$. The bipolaron binding energy is $\Delta = 1.23E_p - V_c - 4(2t + t')$. As in the ladder, the bipolaron already moves in the *first* order in polaron hopping. This remarkable property is entirely due to the strong on-site repulsion and long-range el–ph interaction that leads to a non-trivial connectivity of the lattice. This situation is unlike all other models studied previously. (Usually, the bipolaron moves only in the second order in polaron hopping and therefore is very heavy.) In our model, this fact combines with a weak renormalization of t' yielding a *superlight* bipolaron with mass $m^{**} \propto \exp(0.60E_p/\omega)$. We recall that in the Holstein model $m^{**} \propto \exp(2E_p/\omega)$. Thus the mass of the Fröhlich bipolaron scales approximately as a *cube root* of that of the Holstein one.

At even stronger el–ph interaction, $V_c < 1.16E_p$, NNN bipolarons become stable. More importantly, holes can now form three- and four-particle clusters. The dominance of the potential energy over kinetic energy in Hamiltonian (10) enables us to readily investigate these many-polaron cases. Three holes placed within one oxygen square have four degenerate states with energy $2(V_c - 1.23E_p) + V_c/\sqrt{2} - 0.80E_p$. The first-order polaron hopping processes mix the states resulting in a ground-state linear combination with energy $E_3 = 2.71V_c - 3.26E_p - \sqrt{4t^2 + t'^2}$. It is essential that between the squares such triads could move only in higher orders in polaron hopping. In the first order, they are immobile. A cluster of four holes has only one state within a square of oxygen atoms. Its energy is

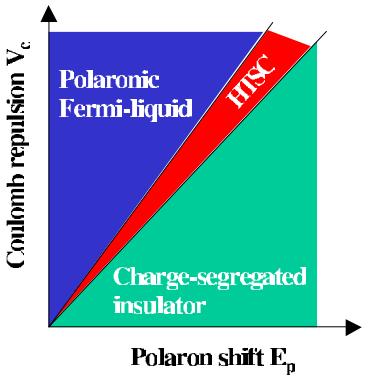

Figure 5. The phase diagram of the Fröhlich–Coulomb model. The model is a polaronic Fermi liquid for the strong Coulomb repulsion, a bipolaronic HTSC for the intermediate Coulomb repulsion, and a charge-segregated insulator for the weak repulsion.

$E_4 = 4(V_c - 1.23E_p) + 2(V_c/\sqrt{2} - 0.80E_p) = 5.41V_c - 6.52E_p$. This cluster as well as all the bigger ones are also immobile in the first order of polaron hopping. We conclude that at $V_c < 1.16E_p$ the system quickly becomes a charge-segregated insulator.

The fact that within the window $1.16E_p < V_c < 1.23E_p$ there are no bound states of three or more polarons means that bipolarons repel each other. The system is effectively the charged Bose gas which is a well known superconductor [7]. The superconductivity window that we have found is quite narrow (see figure 5). This indicates that the superconducting state in such systems is a subtle phenomenon which requires a fine balance between electronic and ionic interactions. Too strong el–ph interaction leads to clustering, while too weak interaction cannot bind the carriers and the superconductivity is at best of BCS type. These considerations may provide additional insight into the uniqueness of one particular structure, the copper–oxygen perovskite layer, for HTSC. It also follows from our model that superconductivity should be very sensitive to any external factor that affects the balance between V_c and E_p. For instance, pressure changes the octahedra geometry and hence E_p and $V_{\rm pa}$. Chemical doping enhances internal screening and consequently reduces E_p.

We now assume that the superconductivity condition is satisfied and show that our Fröhlich–Coulomb model possesses many key properties of the underdoped cuprates. The bipolaron binding energy Δ should manifest itself as a normal-state pseudogap with size of approximately half of Δ [7]. Such a pseudogap was indeed observed in many cuprates. In contrast with the case for the BCS superconductor, the symmetry of the pseudogap might differ from the symmetry of the superconducting order parameter, which depends on the bipolaronic band dispersion. The symmetry of the order parameter was found to be d wave [25], while the former is an anisotropic s wave, in accordance with many experimental observations. There should be a strong isotope effect on the (bi)polaron mass because $t, t' \propto \exp(-\text{constant} \times \sqrt{M})$. Therefore the replacement of O^{16} by O^{18} increases the carrier mass [26]. Such an effect was observed in the London penetration depth of the isotope-substituted samples [1]. The mass isotope exponent, $\alpha_m = \mathrm{d}\ln m^{**}/\mathrm{d}\ln M$, was found to be as large as $\alpha_m = 0.8$ in $La_{1.895}Sr_{0.105}CuO_4$. Our theoretical exponent is $\alpha_m = 0.3E_p/\omega$, so the bipolaron mass enhancement factor is $\exp(0.6E_p/\omega) \simeq 5$ in this material. With the bare hopping integral $T_{NNN} = 0.2$ eV we obtain the in-plane bipolaron mass $m^{**} \simeq 10\,m_e$. Calculated with this value, the in-plane London penetration depth, $\lambda_{ab} = [m^{**}/8\pi ne^2]^{1/2} \simeq 316$ nm (n the hole

density), agrees well with the measured one, $\lambda_{ab} \simeq 320$ nm. Taking into account the c-axis tunnelling of bipolarons, the critical temperature of their Bose–Einstein condensation can be expressed in terms of the experimentally measured in-plane and c-axis penetration depths, and the in-plane Hall constant R_H as $T_c \approx 1.64(eR_H/\lambda_{ab}^4\lambda_c^2)^{1/3}$. Here T_c, eR_H, and λ are measured in K, cm^3, and cm, respectively [27]. Using the experimental $\lambda_{ab} = 320$ nm, $\lambda_c = 4160$ nm, and $R_H = 4 \times 10^{-3}$ cm^3 C^{-1} (just above T_c), one obtains $T_c = 31$ K in striking agreement with the experimental value $T_c = 30$ K. The recent observation of the normal-state diamagnetism in $La_{2-x}Sr_xCuO_4$ [28] also fits well the prediction of the bipolaron theory [29]. Many other features of the bipolaronic (super)conductor, e.g., the unusual upper critical field, electronic specific heat, optical, ARPES, and tunnelling spectra match those of the cuprates (for a recent review, see [30]).

Finally, we show that the Fermi energy in all novel superconductors is surprisingly low, of the order of or even smaller than the most essential optical phonon energy. The band structure of the cuprates is quasi-two-dimensional with a few degenerate hole pockets. Applying the parabolic approximation for the band dispersion one obtains the renormalized (polaronic) Fermi energy as

$$E_F = \frac{\pi n_i d}{m_i^*}, \tag{24}$$

where d is the interplane distance, and n_i, m_i^* are the density of holes and their effective mass in each of the hole subbands i renormalized by the el–ph (and electron–electron) interactions. One can express the renormalized band-structure parameters through the in-plane London penetration depth at $T = 0$, measured experimentally:

$$\frac{1}{\lambda_H^2} = 4\pi e^2 \sum_i \frac{n_i}{m_i^*}. \tag{25}$$

As a result, one obtains the *parameter-free* expression for the Fermi energy as

$$E_F = \frac{d}{4ge^2\lambda_H^2}, \tag{26}$$

where g is the degeneracy of the spectrum. The degeneracy g in the cuprates may depend on the doping. In underdoped cuprates one expects four hole pockets inside the Brillouin zone (BZ) due to the Mott–Hubbard gap. If the hole band minima are shifted with doping to BZ boundaries, the spectrum will be twofold degenerate, so $g \geqslant 2$ in cuprates. Because equation (26) does not contain any other band-structure parameters, the estimate of E_F using this equation does not depend very much on the parabolic approximation for the band dispersion. Generally, the ratios n/m in equations (24) and (25) are not necessarily the same. The 'superfluid' density in equation (25) might be different from the total density of delocalized carriers in equation (24). However, in a translationally invariant system they must be the same [31]. This is true even in the extreme case of a pure two-dimensional superfluid, where quantum fluctuations might be important. One can obtain a reduced value of the zero-temperature superfluid density only in the dirty limit $l \ll \xi(0)$ where $\xi(0)$ is the zero-temperature coherence length. The latter was measured directly in cuprates as the size of the vortex core. It is about 10 Å or even less. In contrast, the mean free path was found to be surprisingly large at low temperatures, $l \sim$ 100–1000 Å. Hence, the cuprates are in the clean limit, $l \gg \xi(0)$, so the parameter-free expression for E_F, equation (26), is perfectly applicable.

Equation (26) yields $E_F \leqslant 100$ meV for the cuprates, especially if the degeneracy $g \geqslant 2$ is taken into account. A few examples are $La_{1.85}Sr_{0.15}CuO_4$ ($T_c = 37$ K, $\lambda_H = 240$ nm [27], $d = 0.66$ nm) with $gE_F = 77$ meV, $YBa_2Cu_3O_{6.92}$ ($T_c = 91.5$ K , $\lambda_H = 186$ nm [27],

$d = 0.43$ nm) with $gE_F = 84$ meV. That should be compared with the characteristic phonon frequency, which is estimated as the plasma frequency of oxygen ions, $\omega = (4\pi Z^2 e^2 N/M)^{1/2}$. One obtains $\omega = 84$ meV with $Z = 2$, $N = 6/V_{\rm cell}$, $M = 16$ au for $YBa_2Cu_3O_6$. Here $V_{\rm cell}$ is the volume of the chemical unit cell. The low Fermi energy $E_F \leqslant \omega$ is a serious problem for the Migdal–Eliashberg approach. The non-crossing diagrams cannot be treated as vertex *corrections* because $\omega/E_F \geqslant 1$, since they are comparable to the standard terms. On the contrary, the estimate of E_F supports further the non-adiabatic (bi)polarons as the (super)carriers in high-T_c superconductors.

In conclusion, we have introduced a realistic multi-polaron model of high-temperature superconductivity with the strong Fröhlich and Coulomb long-range interactions. We have described a simple procedure of calculating polaron and bipolaron masses, identified and quantitatively analysed a new resonance mechanism of bipolaron mass reduction, and found the conditions for clustering of holes and the window for their high-T_c superconductivity. The model possesses a rich phase diagram in the coordinates of the intersite Coulomb repulsion V_c and the polaronic (Franck–Condon) level shift E_p; see figure 5. The ground state is a polaronic Fermi (or Luttinger) liquid for the strong Coulomb repulsion, a bipolaronic HTSC for the intermediate Coulomb repulsion, and a charge-segregated insulator for the weak repulsion. Remarkably, the intersite bipolarons in the superconducting phase are 'superlight', propagating coherently with about the same mass as single polarons. In our model the bipolarons already tunnel in the first order in polaron tunnelling, which results in the bipolaron mass scaling linearly with the polaron hopping integral. Many properties of the model in the superconducting phase match those of the cuprates. We argue that a surprisingly low Fermi energy and the strong unscreened coupling of carriers with high-frequency optical phonons is the origin of the high-temperature superconductivity.

Acknowledgments

This work was supported by the EPSRC, UK (grant R46977), by the Leverhulme Trust (grant F/00261/H), and by DARPA.

References

[1] Zhao G, Hunt M B, Keller H and Müller K A 1997 *Nature* **385** 236
[2] Lanzara A *et al* 2001 *Nature* **412** 510
[3] Timusk T *et al* 1995 *Anharmonic Properties of High-T_c Cuprates* ed D Mihailović *et al* (Singapore: World Scientific) p 171
[4] Egami T 1996 *J. Low Temp. Phys.* **105** 791
[5] Lanzara A *et al* 1999 *J. Phys.: Condens. Matter* **11** L541
[6] Temprano D R *et al* 2000 *Phys. Rev. Lett.* **84** 1982
[7] Alexandrov A S and Mott N F 1994 *Rep. Prog. Phys.* **57** 1197
[8] Devreese J T 1996 *Encyclopedia of Applied Physics* vol 14 (New York: VCH) p 383
[9] Allen P B 2001 *Nature* **412** 494
[10] Gor'kov L P 1999 *J. Supercond.* **12** 9
[11] Bishop A R and Salkola M 1995 *Polarons and Bipolarons in High-T_c Superconductors and Related Materials* ed E K H Salje, A S Alexandrov and W Y Liang (Cambridge: Cambridge University Press) p 353
[12] Fehske H, Loos J and Wellein G 1997 *Z. Phys.* B **104** 619 and references therein
[13] Benedetti P and Zeyher R 1998 *Phys. Rev.* B **58** 14 320
[14] Bonca J, Trugman S A and Batistic I 1999 *Phys. Rev.* B **60** 1633
[15] Proville L and Aubry S 1999 *Eur. Phys. J.* B **11** 41
[16] Alexandrov A S 1996 *Phys. Rev.* B **53** 2863
[17] Alexandrov A S and Bratkovsky A M 2000 *Phys. Rev. Lett.* **84** 2043

[18] Yamashita J and Kurosawa T 1958 *J. Phys. Chem. Solids* **5** 34
and see also
Eagles D M 1969 *Phys. Rev.* **181** 1278
[19] Alexandrov A S and Kornilovitch P E 1999 *Phys. Rev. Lett.* **82** 807
[20] Fehske H, Loos J and Wellein G 2000 *Phys. Rev.* B **61** 8016
[21] Bonca J and Trugman S A 2001 *Phys. Rev.* B **64** 4507
[22] Lang I G and Firsov Yu A 1962 *Zh. Eksp. Teor. Fiz.* **43** 1843 (Engl. transl. 1963 *Sov. Phys.–JETP* **16** 1301)
[23] Alexandrov A S and Ranninger J 1981 *Phys. Rev.* B **23** 1796
[24] Alexandrov A S and Kabanov V V 2000 *JETP Lett.* **72** 569
[25] Alexandrov A S 1998 *Physica* C **305** 46
[26] Alexandrov A S 1992 *Phys. Rev.* B **46** 14 932
[27] Alexandrov A S and Kabanov V V 1999 *Phys. Rev.* B **59** 13 628
[28] Iguchi I, Yamaguchi T and Sugimoto A 2001 *Nature* **412** 420
[29] Dent C J, Alexandrov A S and Kabanov V V 2000 *Physica* C **341–8** 153
[30] Alexandrov A S and Edwards P P 2000 *Physica* C **331** 97
[31] Leggett A J 1973 *Phys. Fenn.* **8** 125